Apparent stress of earthquakes within the shallow subduction zone near Kamchatka Peninsula

Article *in* Bulletin of the Seismological Society of America · June 1996

CITATIONS
11

READS
48

1 author:

Vyacheslav Zobin
Universidad de Colima
224 PUBLICATIONS **1,084** CITATIONS

SEE PROFILE

Bulletin of the Seismological Society of America, Vol. 86, No. 3, pp. 811–820, June 1996

Apparent Stress of Earthquakes within the Shallow Subduction Zone near Kamchatka Peninsula

by Vyacheslav M. Zobin*

Abstract Apparent stresses of 105 moderate-sized (magnitude m_b from 4.5 to 6.0) shallow earthquakes from the subduction zone near Kamchatka Peninsula (NW Pacific) were analyzed. Our results allowed us to formulate the following properties of the earthquake apparent stress for the seismic moment range 10^{15} to 10^{18} N-m and the focal depth range from 0 to 60 km: (1) Apparent stresses depend on the fault nature of earthquakes; they are greater for thrusts and smaller for normal faults, a difference of a factor of 3. (2) Average apparent stresses were greater in the coastal zone near Kamchatka, where subducting oceanic and overriding continental plates interact (2.5 MPa) and just under the trench axis (2.9 MPa), but lower in near-trench zones on the western slope of the trench (0.4 MPa); this difference is a factor of 6.

Introduction

The detailed seismic investigations carried out from 1962 in the Kamchatka-Commander region by the Institute of Volcanology, Russia, yielded a database containing the hypocentral data with a threshold magnitude $m_b = 2$ as well as a set of stress and size parameters of earthquakes (Zobin *et al.,* 1994). In this article, we study the properties of apparent stresses of earthquakes.

As a region of study, we consider a shallow zone where the Pacific plate subducts under the North American plate near Kamchatka Peninsula (Fig. 1). It is a 550-km-long zone at the southern end of Kamchatka Peninsula along the Kurile-Kamchatka ocean trench. Its width is about 250 km, and it has a depth of 60 km. This zone represents the northern end of the Kurile-Kamchatka Island arc to its intersection with the Aleutian structures, represented here by the Commander Islands and the Aleutian trench.

The shallow (focal depth from 0 to 60 km) seismicity in subduction zones accounts for 70% of the annual global seismic energy release (Lay and Wallace, 1995). Shallow subduction processes include the forming of accretionary or erosional wedges and dynamics of the overriding plate. An understanding of processes at shallow depths of subduction zones is very important in terms of plate tectonics.

Our region of study represents one of the most active segments of subduction zones in this century. The great Kamchatkan earthquakes of 1923 (M_S 8.3), 1952 (M_S 8.2), and 1959 (M_S 8.2) occurred within the region (Pacheco and Sykes, 1992). The 1962 to 1991 period was characterized by a rather low level of seismic activity. The largest shallow event of 6 October 1987 had magnitude M_S 6.1 (Zobin *et al.,* 1992).

Figure 2a shows the distribution of earthquake epicenters in 1962 to 1991. They are represented here within two main bands. The first continuous band goes along the coast of Kamchatka. The second band consists of several dense groups of earthquake foci and goes along the western slope of the Kurile-Kamchatka trench. For events of magnitude m_b from 2 to 6, energy release within two bands is of the same order (Fig. 3a). The space between the bands is of rather low activity.

Each of these seismic bands is characterized by a different stress state (Zobin, 1990, 1994; Zobin and Ivanova, 1992, 1994; Zobin and Levina, 1994). The coastal seismic band is characterized by compressive stresses and thrust faulting, seismic foci typically distributed in aftershock-type clusters (Fig. 3b). The near-trench seismic band is characterized by extensional tectonics with strike-slip and normal faultings. Seismic foci in this band have a tendency to distribute in swarm-type clusters (Fig. 3b). The seismic events of the near-trench band are characterized by greater amount of low-frequency radiation compared with those of the coastal band (Zobin and Levina, 1994).

This article is devoted to the study of earthquake apparent stresses within this complex shallow seismic volume. We study spatial distribution of apparent stresses and their dependence upon the earthquake focal mechanism and tectonics.

Methods and Database

Earthquake apparent stresses characterize static stress conditions within the active seismic zone. Apparent stress

*Present address: Observatorio Vulcanologico, Universidad de Colima, Av Universidad 333, Colima, Col. 28030 Mexico.

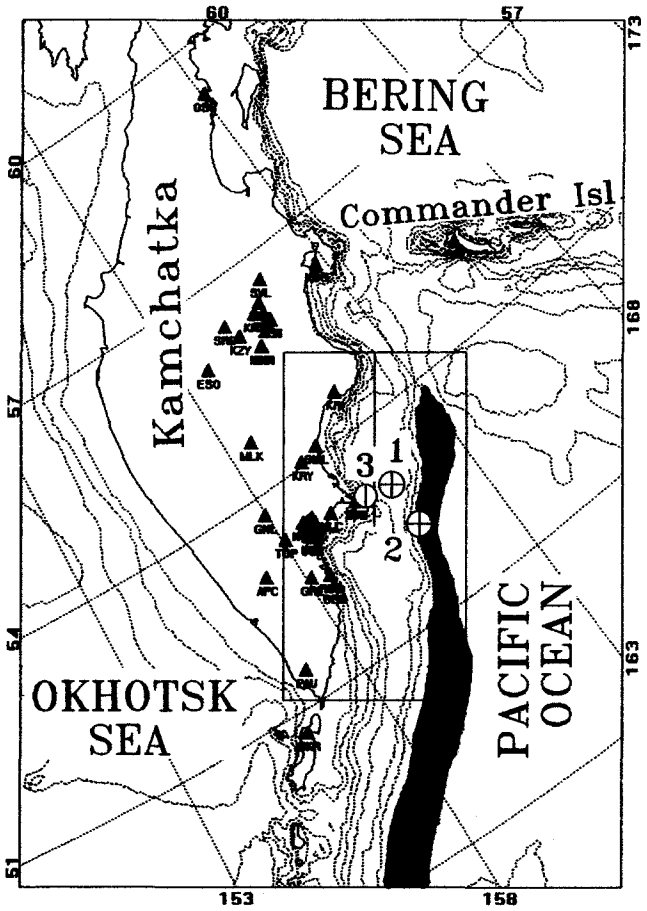

Figure 1. Map of the Kamchatka-Commander region. The regional seismic network is shown by triangles. The frame shows the region of study. The axial part of the Kurile-Kamchatka trench is shown by black space. Three great earthquakes that occurred within the region of study in this century are also shown (1: 02.03, 1923, M_S 8.3; 2: 11.04, 1952, M_S 8.2; 3: 05.04, 1959, M_S 8.2).

$\eta\sigma$ is the product of the seismic efficiency η and the mean stress σ and defines the strength of rock within the earthquake source (Wyss, 1970a). Apparent stress $\eta\sigma$ may be determined as

$$\eta\sigma = \mu \times E/M_0, \tag{1}$$

where E is the energy of the earthquake, radiated as seismic waves, in Joules; M_0 is the seismic moment, in N-m; and μ is the rigidity, in N/m^2.

The μ values depend on focus depth and are listed in Table 1. Seismic energy E was determined in the following way. The catalog of Kamchatkan earthquakes has as a basic size value an energy class KS. It was introduced by Fedotov (1972) and represented an estimate of log E in Joules. Energy class was calculated from the ratio of maximum displacement amplitude of S waves of earthquakes, recorded by regional short-period (T_s = 1.2 sec) seismic network with magnification from 250 to 10,000, to the period of these oscillations. A special nomogram proposed by Fedotov (1972) was based on empirical determination of the distance attenuation function and allowed to calculate energy class KS of Kamchatkan earthquakes with depths ranging from 0 to 200 km at distances ranging from 10 to 1000 km. After applying station corrections, mean error for estimation of KS by records of six and more stations is ± 0.3 (Zobin *et al.*, 1993). We use this parameter KS for estimation of seismic energy.

In seismological practice, energy radiated by seismic waves may be calculated either from the integral of squared velocity or from determination of the source function by inversion of seismograms or from any regression equations. The most popular relation is the one by Gutenberg and Richter (1956) between energy E and the surface-wave magnitude M_S:

$$\log E = 1.5\, M_S + 4.8 \ (E \text{ in Joules}). \tag{2}$$

For better understanding of the physical sense of energy class KS, we could represent it in the same form. The regression between KS and M_S (Fig. 4) gives us

$$KS = 1.5\, M_S + 5.1. \tag{3}$$

From (2) and (3),

$$\log E = KS - 0.3, \tag{4}$$

or

$$E = 0.5 \times 10^{KS} \text{ (Joules)}. \tag{5}$$

Equation (4) is a result of combining two empirical relationships, and its quality is rather low for estimation of the absolute value of energy. Nevertheless, it may be useful for study of the variations in energy and other related parameters within the Kamchatkan region.

Comparison between estimations of seismic energy E from equation (5) and estimations calculated with the Boatwright and Choy (1986) method—when energy flux in the P waves was integrated directly, for 5 Kamchatkan earthquakes (*Bulletin of ISC*)—shows a good coincidence of both types of estimations (Table 2) with mean difference log $E_$ISC $-$ log $E\_KS = -0.12$, or less than a factor of 2.

The next parameter that was used for estimation of apparent stress is the scalar seismic moment M_0. We calculated seismic moment from spectral density of Rayleigh seismic waves recorded by three intermediate-period seismic stations (T_s = 20 sec): Petropavlovsk (PET), Severo-Kurilsk (SKR), and Stekolny (MA1), which are situated at distances from 150 to 1500 km of the epicenters. An example of the Rayleigh-wave record and its spectrum is presented in Figure 5. The seismic moment was calculated according to Harkrider's model (Harkrider, 1970):

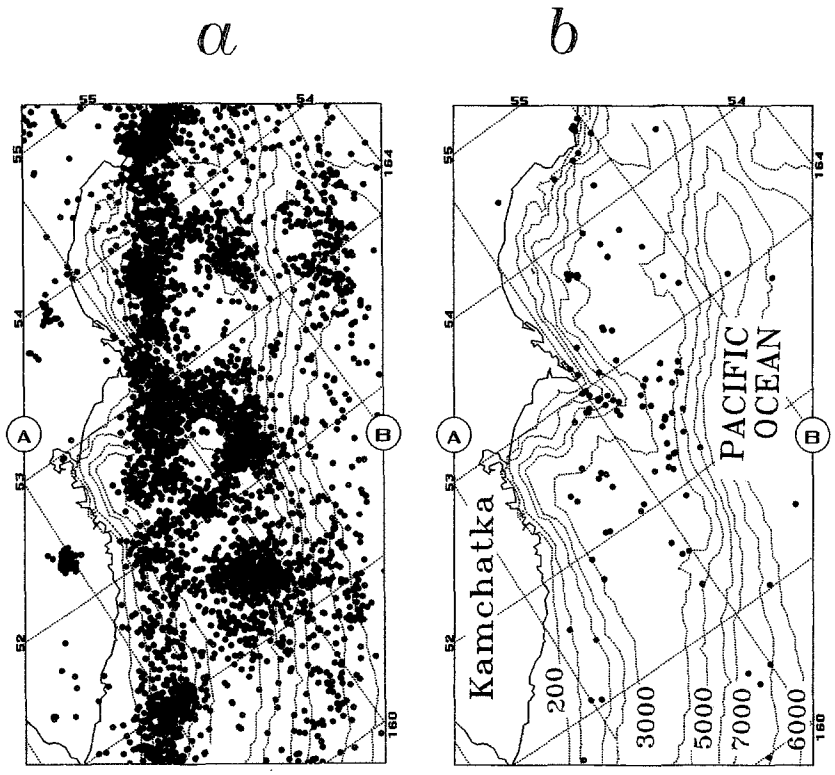

Figure 2. Epicenters of earthquakes near Kamchatka Peninsula, depth range from 0 to 60 km. (a) 1962 to 1991, energy range KS = 9.5 to 15 (m_b = 3 to 6.5); (b) 1979 to 1991, events used in this study. The first map (a) gives more common representation of the epicentral field in the region. Two bands of seismicity, one along the coast and another along the trench slope, are distinctively seen. Bathymetry in meters is also shown. A-B, line of profile.

$$M_0 = \frac{U_r \sqrt{2\pi \times C_r \times \Delta \exp[\gamma_r \times \Delta]/T_r}}{\varepsilon_0 \times A_r \chi(\theta, h)}, \qquad (6)$$

where T_r is the period at which the spectral density U_r is calculated, h is the focal depth, Δ is the epicentral distance, A_r is the Rayleigh-wave amplitude factor, ε_0 is the Earth ellipcity correction, $\chi(\theta, h)$ is the radiation pattern, γ_r is the attenuation constant, and C_r is the Rayleigh-wave phase velocity. Parameters for calculating the radiation pattern and parameters A_r, γ_r, C_r, and ε_0 were taken from standard tables (Harkrider, 1970) and focal mechanism solutions. Seismic moments were calculated for spectral density at periods 30, 25, and 20 sec (see Fig. 5), and then they were averaged.

Comparison of our 36 estimates of seismic moment with Harvard scalar seismic moments, taken from *Harvard CMT Data Base,* shows that these two estimates are similar and that mean difference between log M_0_HAR and log M_0_KAM is 0.07 $\pm$ 0.27. We will take a value of $\pm$0.3 in log unit as an error for our estimations of seismic moments. Due to estimated errors for KS ($\pm$0.3) and log M_0 ($\pm$0.3 log unit), we could consider our estimations of apparent stress with a multiplicative error factor of 4.

We calculated 105 apparent stresses for events of the 1979 to 1991 period, that is, 58% of all the events that occurred in the range of energy class KS = 11.5 to 13.5, magnitude m_b = 4.5 to 6.0, and depth range 0 to 60 km. Their epicenters are shown in Figure 2b; the list of data is presented in an appendix. We omitted the greater events to avoid effects of saturation. All events were located using the regional short-period seismic network with application of the local time-distance curves (Kuzin, 1974). Errors in epicenter location are 3.0 km, and in depth determination, 5.0 km.

Focal mechanisms were determined from distribution of the first *P*-wave motions taken from records of Kamchatkan regional seismic network and from worldwide data published by *ISC.*

Distribution of Apparent Stresses across a Shallow Subduction Zone

Figure 6 shows a cross section with apparent stress estimations across the shallow subduction zone near Kamchatka. Apparent stresses are represented for four orders of magnitude, from 0.01 up to 32 MPa. They are characterized by a weak dependence upon the depth (coefficient of correlation R = 0.48) and the earthquake size (for seismic moment, R = 0.51; for magnitude m_b, R = 0.20). This allows us to discuss the distribution of apparent stress without any correction for the focal depth and earthquake size.

Table 1
Dependence of the Rigidity upon Depth Used for the Calculation of Apparent Stress

Depth (km)	Rigidity (10^{10} N/m^2)
0	3.5
20	4.2
35	6.0
60	7.9

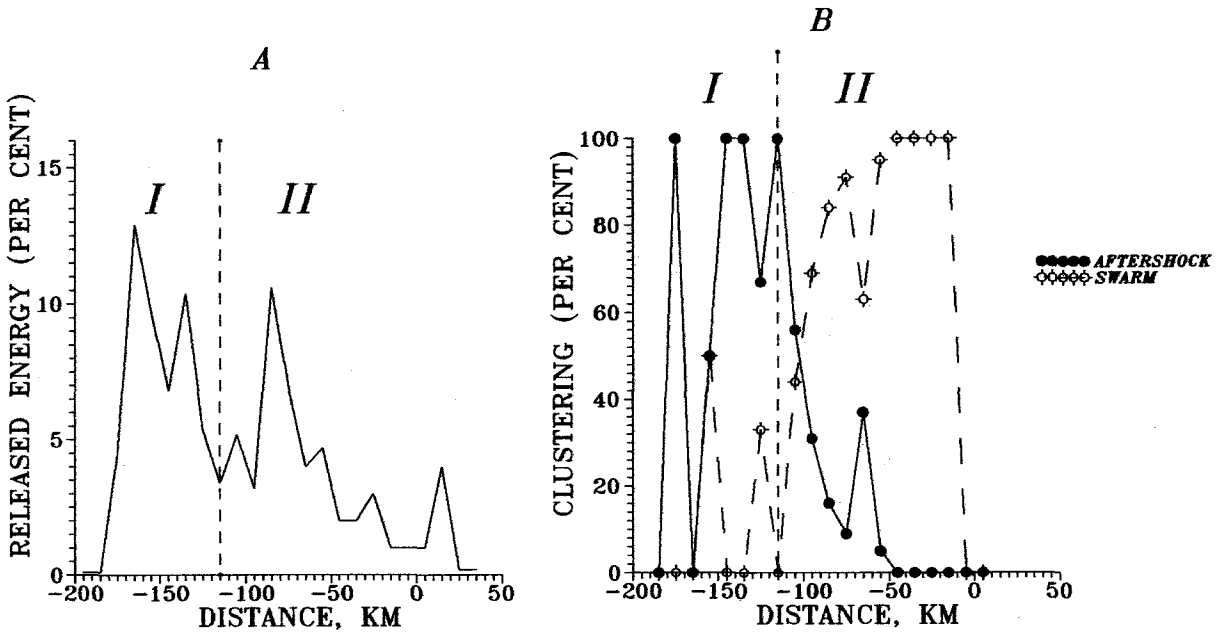

Figure 3. Variations of earthquake properties across the shallow subduction zone (along the profile A-B from Fig. 2a). (a) Energy release across the shallow subduction zone in 1962 to 1991 for each 10 km of distance, in percentage of total energy release, for events of magnitude m_b range from 4.5 to 6. (b) Distribution of two types of earthquake clusters, swarms and mainshock–aftershock sequences, across the shallow subduction zone, in percentage of all events of magnitude $m_b \geqq 4.5$ that occurred in these clusters. I and II indicate activity related to coastal (I) and near-trench (II) seismic bands. The distance is measured from the axis of the trench. The distribution of two types of earthquake clusters is based on the definition of the swarm and mainshock–aftershock sequences for the Kamchatkan region given in (Zobin and Ivanova, 1992, 1994). In Kamchatka, 42% of all events of magnitude $\geqq 5.5$ during 1962 to 1991 occurred within clusters, and this distribution is an important characteristic of the stress state in the region.

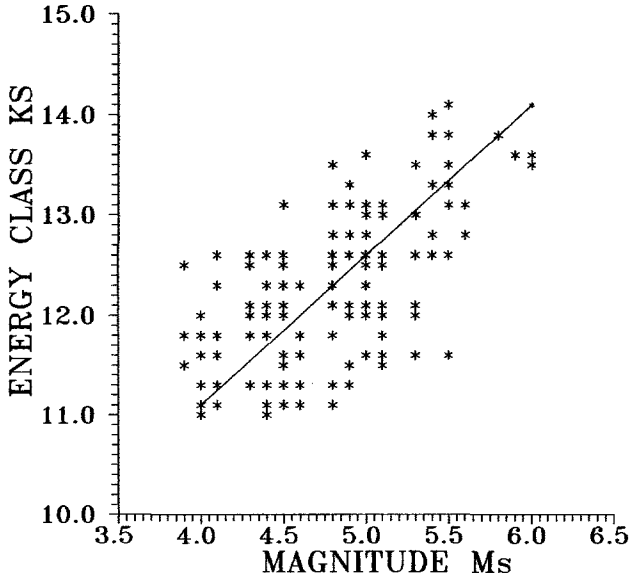

Figure 4. Relationship between the energy class *KS* and magnitude M_S.

Table 2

Comparison of Earthquake Energy Estimations from Energy Class *KS* and by the Boatwright and Choy (1986) Method

Date (yymmddhhmm)	Depth (km)	*KS*	M_0_HAR (N-m)	log *E*_ISC (N-m)	log *E_KS* (N-m)
8710062011	34	13.9	6.2×10^{18}	13.4	13.6
9012191348	24	13.5	9.5×10^{17}	12.8	13.2
9203021229	20	14.6	2.3×10^{19}	14.1	14.3
9203051439	31	14.0	3.7×10^{18}	13.7	13.7
9212191214	40	13.4	1.3×10^{18}	13.3	13.1

Note: M_0_HAR, scalar seismic moment estimated by Harvard group; log *E*_ISC, logarithm of seismic energy estimated by the Boatwright and Choy (1986) method (both these values were published in *ISC*); log *E_KS* = *KS* − 0.3.

For the sake of clarity, we consider apparent stress values from 0.01 up to 0.99 MPa as small values and from 1.0 up to 100 MPa as large values. One can see that there is good discrimination in cross section between zones with small and large apparent stresses. Zone I, near the coast of Kamchatka, is characterized by a predominance of large apparent stresses, while the near-trench zone II is characterized by a predominance of small apparent stresses. Within zone

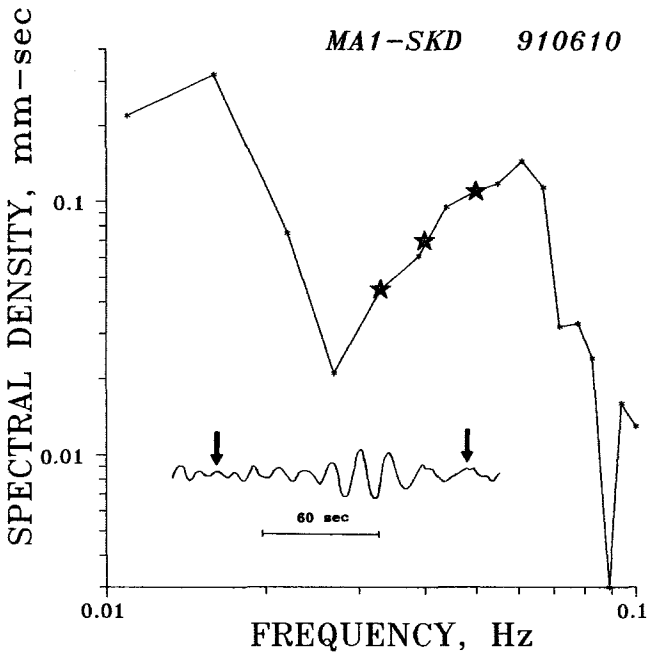

Figure 5. Example of the Rayleigh-wave record by intermediate-period seismograph SKD of Kamchatkan earthquake at epicentral distance of 950 km and its spectrum. Arrows show length of sample for digitizing. Stars indicate spectral densities at periods of 20, 25, and 30 sec. Spectrum is corrected for the instrument response.

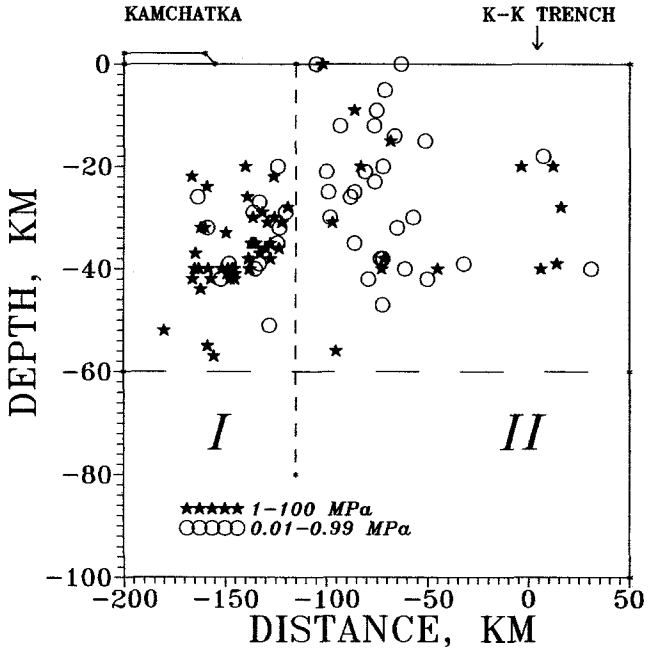

Figure 6. Distribution of apparent stresses across the shallow subduction zone (along profile A-B from Fig. 2b). I and II indicate two bands of seismicity: coastal (I) and near-trench (II). Stars show events with large apparent stress (1 MPa and greater); circles show events of smaller apparent stress (less than 1 MPa). Distance is measured from the axis of the trench, which is shown by an arrow. The dashed line shows the border between bands I and II.

II, it is possible to see a dense group of five events with large apparent stresses just under the axis of the trench (on the right side of Fig. 6). Calculation of the mean values of apparent stresses for both zones gives a significant difference between them due to *t*-test of difference between two means (chapter IV.4 from Beyer, 1985). For zone I, a mean geometrical value is 0.39 ± 0.45 log unit MPa for 55 events (or 2.5 MPa), and for zone II (without five events under the trench), it is −0.37 ± 0.56 log unit MPa for 50 events (or 0.43 MPa), or the difference is a factor of about 6. For the group under the trench, the mean value is 2.9 MPa for five events.

Apparent Stresses and Focal Mechanisms

Figure 7 shows a cross section across the subduction zone with indications of different nature of fault for the events that were represented in the cross section of Figure 6. We use three gradations of fault nature according to different values of the fault slip: strike slip, if slip is in the range of 0° to 20° or 161° to 180°; thrust (or normal fault), if slip is in the range of 71° to 110° (or from −71° to −110°); and strike slip with thrusting (or normal faulting) component, if slip range is in the range of 20° to 70° and 111° to 160° (or from −20° to −70° and from −111° to −160°). In Figure 7, events of thrusts and strike slip with thrusting component (or of normal fault and strike slip with normal-faulting component) are marked by the same symbols. One can see good discrimination between coastal and near-trench events. For coastal events, thrusting is the dominating type of faulting (76% of all events), and normal faults represent only 5%. At the same time, for near-trench events, normal faults and strike slips are dominating (63% of all events). It is interesting to observe that the limit between zones I and II, which divided (in Fig. 6) events with high and low apparent stresses, is the same for dividing events with a different fault nature. So we can say that events with high apparent stresses were originated in media with predominance of horizontal compression, while the low apparent stress events occurred in media with predominance of horizontal tension. A plot of data for pure thrusts and normal faults (Fig. 8a) shows this effect more distinctly. To avoid an influence of dependence upon earthquake size, all data are represented only for one order of seismic moment. We can see a significant difference between apparent stresses of events with a different fault nature. The mean geometrical value of apparent stresses for normal faults is −0.10 ± 0.09 log unit MPa for four events (or 0.79 MPa) and for thrusts, 0.39 ± 0.46 log unit MPa for 14 events (or 2.45 MPa), or 3.2 times greater for thrusts. Although the difference between apparent stresses for thrusts and strike slips (Fig. 8b) may be noted, they are not so significant.

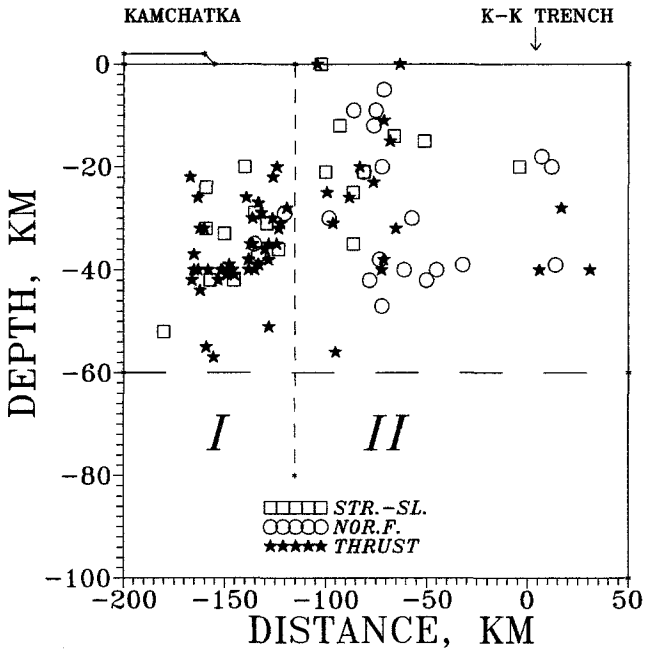

Figure 7. Distribution of events with different fault nature across the shallow subduction zone (along profile A-B from Fig. 2b). I and II indicate two bands of seismicity: coastal (I) and near-trench (II). The square shows strike slip, the circle shows normal fault, and the star shows thrust faulting. Distance is measured from the axis of the trench, which is shown by an arrow. The dashed line shows the limit between bands I and II.

Results and Discussion

The study of apparent stresses for intermediate-sized shallow earthquakes that occurred within the Kamchatkan subduction zone in the depth range from 0 to 60 km shows that for events of seismic moments from 10^{15} to 10^{18} N-m, apparent stresses vary from 0.01 to 32 MPa.

Wyss (1970a) defined the apparent stress as a lower bound for the average stress acting in the source region. Liu and McNally (1993) obtained shear stresses at the interplate contact for Kamchatka of the order of 30 MPa, which is close to our higher estimates.

Our results yield the following properties of the earthquake apparent stress for the seismic moment range 10^{15} to 10^{18} N-m:

1. Apparent stresses depend on fault nature of earthquakes: they are greater for thrusts and smaller for normal faults.
2. Apparent stresses are greater in the coastal zone near Kamchatka, where subducting oceanic and overriding continental plates interact, and just under the trench axis but lower in the near-trench zone on the western slope of the trench.

Boore (1986) proposed a model that predicts a dependence of apparent stress on moment, with an abrupt transition (at $M_0 = 10^{12}$ to 10^{14} N-m) to an approximately constant level for the range of $M_0 = 10^{14}$ to 10^{20} N-m. Figure 9 shows Boore's curve calculated for media with intermediate attenuation. We compare our data with that obtained by different authors. Here we include our data with the estimations of earthquake apparent stress for Mexican (Rebollar *et al.*, 1991), Aleutian (Scherbaum and Kisslinger, 1984; Wyss, 1970b), Kurile (Hanks, 1971), and South American (Wyss, 1970a) subduction zones together with relatively large Hawaiian (Zuñiga *et al.*, 1987) and small Cal-

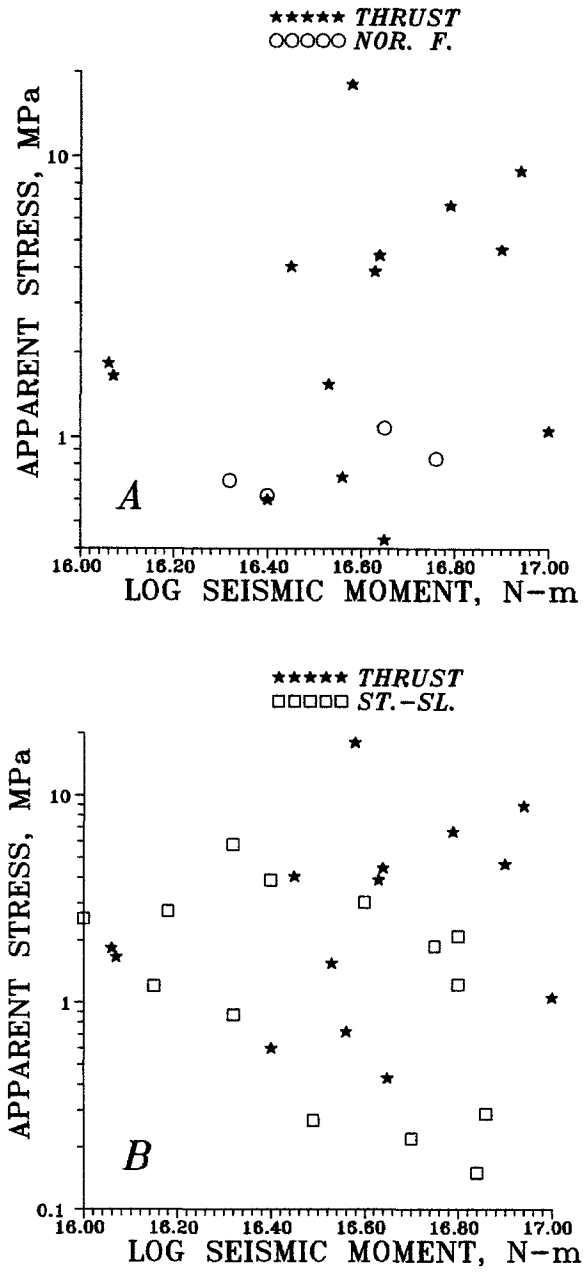

Figure 8. Dependence of apparent stress upon the fault nature: (a) thrust and normal faults and (b) thrust and strike slips. Thrust is shown by the star; normal faults are shown by the circle, and strike slip is shown by the square.

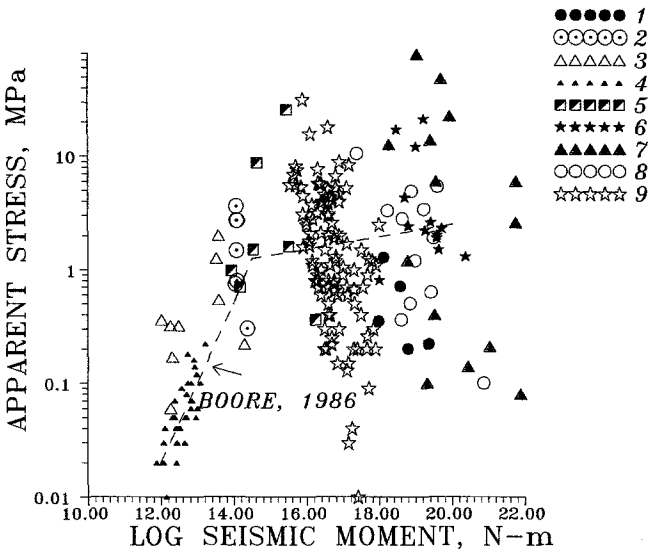

Figure 9. Scaling law for apparent stress. Boore's law for intermediate attenuation media is shown by the dashed line. 1, large Kamchatkan events from Table 2; 2, Hawaiian events of seismic moment larger than 10^{14} N-m (Zuñiga *et al.*, 1987); 3, Californian events (Abercrombie, 1995); 4, Aleutian events, Adak (Scherbaum and Kisslinger, 1984); 5, events of Oaxaca, Mexico (Rebollar *et al.*, 1991); 6, South American events (Wyss, 1970a); 7, Kurile events (Hanks, 1971); 8, Aleutian events (Wyss, 1970b); and 9, Kamchatkan events (this study).

ifornian earthquakes (Abercrombie, 1996). One can see that small Californian and Aleutian earthquakes are well fitted by Boore's curve. For this moment interval, from 10^{12} to 10^{14} N-m, apparent stress increases with moment. At the same time, for larger seismic moments, such dependence is absent. Our set of apparent stresses for moderate-sized shallow Kamchatkan earthquakes is close in its range to apparent stresses estimated for other subduction zones.

Wyss (1970b) proposed a value about 2 MPa as the average apparent stress for shallow events from different regions. Figure 9 shows that this value is rather realistic for events of seismic moment greater than 10^{14} N-m. From this point of view, we could consider that apparent stresses overall do not depend upon seismic moment for moments greater than 10^{14} N-m; however, for each region, there may exist local specific scaling. Therefore, it is possible to take Boore's curve as the average one for all sets of data, considering that complex structure of focal zones may produce a great dispersion of stress estimations and local regularities in scaling.

Dependence of apparent stresses on focal mechanism was noted earlier by Cocco and Rovelli (1989). They had studied stress drops and apparent stresses for normal- and thrust-faulting events in Italy and found that the thrust-faulting events had stress values 2 to 3 times larger than those for normal faults, which is in good accordance with our data.

This difference in apparent stresses for events that occurred under action of horizontal tension or compression naturally produces the difference in apparent stresses acting in the coastal compressive band (high apparent stress) and extensional near-trench band (low apparent stress) of the subduction zone. These two bands are characterized by significant difference in earthquake source properties, not only for Kamchatka but also along all NW Pacific subduction zones until Honshu.

For the Kamchatkan region, swarm sequences are well developed along the trench slope, and aftershock sequences occur mainly along the coast of Kamchatka; the area of swarm events is one order larger than those of mainshock–aftershock sequences for the same magnitude of main events (Zobin, 1995). Results of other authors show that this regularity in existence of two parallel seismic belts with difference in source properties is valid for the Kurile and Japanese earthquakes too. Mogi (1967) showed that a seismic band along the Japan trenches is characterized by swarm activity, while there is a domination of aftershock activity along the coastal part of Japan. Schwartz and Ruff (1987) have studied large Kurile earthquakes of the 1947 to 1985 period and showed that there were two types of events: low-stress-drop events with long aftershock area and source time function of about 40 sec that occurred along the trench slope (swarm-type sequences?) and impulsive events with a small area of aftershocks and more short source time functions of about 16 sec, which were situated along the coast of the Kurile Islands. This tends to support our results and suggests differences in the stress state for the near-trench and coastal zones of the northwestern Pacific subduction zones. In the context of plate tectonics, it may be related to existence of a well-developed band of accretional wedges on the slopes of the system of Kurile-Kamchatka and Japan trenches that may be a focal zone for low-apparent-stress events with extensive fault area.

Our average estimates of apparent stress for different parts of subduction zone [large for coastal part (2.5 MPa) and just under the trench axis (2.9 MPa), but small for events that were situated along the trench slope (0.43 MPa)] are comparable with apparent stresses estimated for the region of the Kurile trench (to the south from our region of study) by Hanks (1971). Hanks presented apparent stresses for 14 events of seismic moment from 10^{18} to 10^{21} N-m. Two of them occurred along the trench axis, their average apparent stress being 50 MPa; two occurred along the trench slope, their average apparent stress being 0.3 MPa; and the other 10 events occurred along the coastal zone, their average apparent stress being 2.8 MPa. These estimations of average apparent stresses for the trench slope and the coastal zone are very close to ours.

Conclusions

Analysis of apparent stresses estimated for moderate-sized shallow Kamchatkan earthquakes shows that apparent stresses depend on the type of earthquake fault. They reflect

differences in stress states within subduction zones; stresses are evidently larger in the coastal part of a subducting zone where two plates interact, but lower within the near-trench slope.

Acknowledgments

The database for this article was prepared while I was at the Institute of Volcanology, Russia. I thank V. Levina, V. Chirkova, and S. Mityushkina for their help in preparation and organization of the database. I am grateful to Drs. R. Castro, H. Fabriol, A. McGarr, and R. Zuñiga and to two anonymous reviewers for valuable advice and critical reading of the manuscript.

References

Abercrombie, R. E. (1996). Earthquake source scaling relationships from −1 to 5 ML using seismograms recorded at 2.5 km depth, *J. Geophys. Res.* (in press).

Beyer, W. H. (1985). *Handbook of Tables for Probability and Statistics,* CRC Press, Inc., Boca Raton, Florida, 642 pp.

Boatwright, J. and G. L. Choy (1986). Teleseismic estimates of the energy radiated by shallow earthquakes, *J. Geophys. Res.* **91,** 2095–2112.

Boore, D. M. (1986). The effect of finite bandwidth on seismic scaling relationships, in *Earthquake Source Mechanics,* S. Das, J. Boatwright, and C. H. Scholz (Editors), Geophys. Monog. 37, American Geophysical Union, Washington, D.C., 275–283.

Cocco, M. and A. Rovelli (1989). Evidence for the variation of stress drop between normal and thrust faulting earthquakes in Italy, *J. Geophys. Res.* **94,** 9399–9416.

Fedotov, S. A. (1972). *Energy Classification of Kamchatkan Earthquakes and the Problem of Magnitudes,* Nauka, Moscow, 116 pp. (in Russian).

Gutenberg, B. and C. F. Richter (1956). Earthquake magnitude, intensity, energy, and acceleration, *Bull. Seism. Soc. Am.* **46,** 105–145.

Hanks, T. C. (1971). The Kuril trench—Hokkaido rise system: large shallow earthquakes and simple models of deformations, *Geophys. J. R. Astr. Soc.* **23,** 173–189.

Harkrider, D. G. (1970). Surface waves in multilayed elastic media II. Higher mode spectra ratios from point sources in plane layered earth model, *Bull. Seism. Soc. Am.* **60,** 1937–1987.

Kuzin, I. P. (1974). *The Focal Zone and Upper Mantle Structure of the East Kamchatka,* Nauka, Moscow, 127 pp. (in Russian).

Lay, T. and T. C. Wallace (1995). *Modern Global Seismology,* Academic Press, San Diego, 521 pp.

Liu, X. and K. C. McNally (1993). Quantitative estimates of interplate coupling inferred from outer rise earthquakes, *Pageoph* **140,** 211–237.

Mogi, K. (1967). Regional variation of aftershock activity, *Bull. Earthquake Res. Inst.* **45,** 711–726.

Pacheco, J. F. and R. L. Sykes (1992). Seismic moment catalog of large shallow earthquakes, 1900 to 1989, *Bull. Seism. Soc. Am.* **82,** 1306–1349.

Rebollar, C. J., L. Munguia, A. Reyes, A. Uribe, and O. Jimenez (1991). Estimates of shallow attenuation and apparent stresses from aftershocks of the Oaxaca earthquake of 1978, *Bull. Seism. Soc. Am.* **81,** 99–108.

Scherbaum, F. and C. Kisslinger (1984). Variations of apparent stresses and stress drops prior to the earthquake of 6 May 1984 (mb = 5.8) in the Adak seismic zone, *Bull. Seism. Soc. Am.* **74,** 2577–2592.

Schwartz, S. Y. and L. J. Ruff (1987). Asperity distribution and earthquake occurrence in the southern Kurile Islands arc, *Phys. Earth Planet. Interiors* **49,** 54–77.

Wyss, M. (1970a). Stress estimates for South American shallow and deep earthquakes, *J. Geophys. Res.* **75,** 1529–1544.

Wyss, M. (1970b). Apparent stresses of earthquakes on ridges compared to apparent stresses of earthquakes in trenches, *Geophys. J. RAS* **19,** 479–484.

Zobin, V. M. (1990). Earthquake focal mechanisms and seismotectonic deformations in the Kamchatka-Commander region, *J. Geodyn.* **12,** 1–19.

Zobin, V. M. (1994). Structure and activity of seismic volume at the subduction zone near Kamchatka (abstract), *Seism. Res. Lett.* **65,** 60.

Zobin, V. M. (1995). Earthquake clustering near Kamchatka peninsula and quantification of the earthquake cluster area (abstract), *XXI Gener. Assemb.,* Boulder, Colorado, B339.

Zobin, V. M., E. I. Gordeev, V. F. Bakhtiarov *et al.* (1992). Seismic hazard monitoring in Kamchatka and its applications to the M = 6.6 earthquake of 6 October 1987, *Natural Hazard* **6,** 51–70.

Zobin, V. M. and E. I. Ivanova (1992). Aftershocks of shallow earthquakes near Kamchatka Peninsula. *Geophys. J. Int.* **108,** 749–757.

Zobin, V. M. and E. I. Ivanova (1994). Earthquake swarms in the Kamchatka-Commander Region, *Geophys. J. Int.* **117,** 33–47.

Zobin, V. M. and V. I. Levina (1994). Dependence of relationship between an energy class and magnitude of earthquakes in the Kamchatka-Commander region upon the regional stress, *Volcanol. Seism.* **4–5,** 116–120 (in Russian).

Zobin, V. M., V. I. Levina, and T. S. Lepskaya (1994). *Data Base of the Kamchatkan Earthquakes, 1962–1993,* Institute of Volcanology, Petropavlovsk-Kamchatsky (unpublished).

Zobin, V. M., S. V. Mityushkina, and V. N. Chirkova (1993). Station corrections to S. A. Fedotov's nomograms for the energy classification of earthquakes in Kamchatka and Commander Islands, *Volcanol. Seism.* **1,** 82–92 (in Russian).

Zuñiga, F. R., M. Wyss, and M. E. Wilson (1987). Apparent stresses, stress drops, and amplitude ratios of earthquakes preceding and following the Hawaii Ms = 7.2 mainshock, *Bull. Seism. Soc. Am.* **77,** 69–96.

Division Ciencias de la Tierra
CICESE, Ensenada, B.C.
22800 Mexico

Manuscript received 2 February 1995.

Appendix

Catalog of Kamchatkan Earthquakes (1979–1991, h = 0–60 km, KS = 11.5–13.4)

Date (y m d)	Time (h m s)	Lat. (N)	Lon. (E)	*h* (km)	KS	*mb*	Log M_0 (N-m)	Slip (deg)	Ap. Str. (MPa)
790115	204302.1	51.43	158.43	037	12.2	4.9	16.29	−030	03.6
790117	190941.2	52.88	160.08	040	12.3	5.2	16.58	+147	02.0
790207	010152.0	51.60	158.23	040	11.7	5.0	15.54	+094	05.6
790320	043459.4	50.58	159.72	020	11.9	5.1	16.15	−011	01.2
790523	004041.6	50.46	159.77	018	12.7	5.7	17.66	−068	00.2

Appendix

Continued

Date (y m d)	Time (h m s)	Lat. (N)	Lon. (E)	h (km)	KS	mb	Log M_0 (N-m)	Slip (deg)	Ap. Str. (MPa)
790625	184552.2	52.74	160.20	031	12.7	5.3	16.46	+131	04.6
790829	051211.3	52.43	159.61	039	11.6	4.8	16.41	+095	00.6
790901	175454.1	52.70	161.09	011	12.4	5.5	17.40	+147	00.2
790901	230722.5	52.83	160.98	025	11.9	5.0	16.86	−002	00.3
790902	075954.6	52.76	161.17	005	12.4	5.3	16.85	−048	00.6
791115	161936.6	52.40	159.65	031	12.2	4.9	16.18	−165	02.8
800123	023410.4	52.23	160.40	014	13.4	5.6	18.03	+167	02.5
800123	081226.4	52.23	160.50	038	13.2	5.7	17.69	+084	01.3
800123	082253.3	52.23	160.48	040	12.7	5.3	16.58	+127	05.1
800123	100710.6	52.17	160.33	023	12.5	5.3	17.13	+155	00.6
800123	115602.9	52.32	160.48	042	12.4	5.0	17.05	−146	00.9
800124	065547.0	52.14	160.37	020	12.3	5.0	17.68	−045	00.1
800131	145714.8	52.15	160.79	042	12.1	5.2	16.76	−093	00.8
800211	152945.4	53.12	160.05	057	12.7	5.5	16.64	+106	04.4
800217	190235.5	52.42	159.13	055	12.6	5.5	16.43	+118	05.7
800708	151636.7	52.54	159.44	033	12.7	4.9	16.80	+176	02.1
800910	210926.2	52.99	160.01	041	11.7	5.1	16.07	+104	01.7
801204	104626.8	52.21	160.17	026	13.2	5.5	17.67	+135	00.9
810105	055744.0	54.19	161.61	040	12.8	5.2	15.88	+125	31.7
810201	224328.7	53.06	162.32	039	12.8	5.9	17.55	+064	00.7
810405	020430.5	52.86	159.87	039	11.9	4.9	15.65	+087	06.9
810625	014754.9	52.85	159.90	042	12.5	5.1	16.32	−007	05.8
810731	210653.7	51.08	157.99	040	12.5	5.2	17.68	+097	00.3
811214	091930.3	53.72	160.76	040	12.6	5.4	16.58	+138	04.1
820108	183540.5	53.28	160.64	035	12.2	4.9	15.74	−036	07.6
820120	093033.5	52.49	160.65	021	12.4	5.5	17.41	−001	00.01
820120	110003.6	52.47	160.62	021	12.2	5.1	16.74	−053	00.8
820308	151631.2	52.89	160.08	038	12.6	5.6	16.31	+120	07.7
820720	151149.8	54.43	161.58	037	12.7	5.5	16.09	+066	15.8
830115	004955.7	52.82	160.23	030	12.9	5.6	17.31	+152	01.1
830208	050927.5	51.59	159.87	000	11.5	5.0	17.15	+095	00.03
830208	065839.7	51.58	159.96	030	12.9	5.7	17.84	±033	00.3
830319	114624.7	51.70	159.84	047	11.6	5.3	16.40	−078	00.6
830404	190423.7	52.95	160.02	040	13.1	6.0	17.52	+107	01.5
830407	225656.4	54.40	161.24	052	12.5	5.1	16.59	−173	03.1
830415	145157.0	53.30	160.64	030	12.8	5.8	16.63	+108	03.9
830805	003347.5	52.87	159.73	041	12.6	5.5	16.88	+121	02.0
830822	123908.5	53.73	160.76	024	12.6	5.4	16.75	−010	01.9
840305	065849.7	51.02	160.53	020	13.0	5.6	17.10	−064	01.7
840326	200904.4	50.54	159.99	039	12.0	5.2	15.93	−052	04.5
840506	082121.4	53.04	160.55	036	12.3	5.0	16.81	−002	01.2
840617	081034.8	54.51	160.47	038	11.6	4.9	16.31	−034	00.8
840618	130646.9	52.85	159.68	042	12.4	5.3	16.40	−018	03.9
840902	042001.7	52.05	159.25	035	11.6	5.0	16.16	+132	01.1
850410	203735.3	49.98	159.38	028	13.1	5.5	16.92	+140	04.0
850418	000632.3	52.03	159.75	025	12.8	5.7	17.94	+101	00.2
850418	040648.7	52.06	159.83	031	11.7	4.9	15.91	+117	01.6
050525	232922.8	53.95	161.13	033	13.4	5.9	17.10	−054	05.3
850602	170313.5	52.32	160.73	032	12.6	5.2	17.32	+098	00.5
850603	120507.7	52.44	160.55	020	12.1	4.9	16.10	+134	02.1
850717	121324.7	51.93	160.31	040	11.6	5.1	16.61	+067	00.4
850717	203116.8	52.04	159.30	035	12.0	5.4	16.56	+106	00.7
851117	073031.3	53.75	160.70	026	12.0	5.1	16.43	+150	01.0
860419	175644.1	53.23	161.75	038	11.5	5.1	16.68	+068	00.3
860429	034117.4	52.65	160.49	021	11.6	4.9	16.32	+168	00.9
860522	141014.0	52.78	160.28	029	11.5	5.1	16.32	−088	00.7
860617	004239.3	53.78	160.66	040	13.5	5.9	17.17	+125	08.4
860813	043750.3	52.99	159.96	040	12.0	5.4	15.85	+121	04.5
860821	063712.0	53.74	160.63	022	12.5	5.4	16.80	+147	01.3
860921	233817.6	52.87	160.21	036	12.0	5.1	15.67	+095	08.2
860926	202934.3	52.83	162.73	040	11.9	4.9	15.74	+155	04.5

Appendix
Continued

Date (y m d)	Time (h m s)	Lat. (N)	Lon. (E)	h (km)	KS	mb	Log M_0 (N-m)	Slip (deg)	Ap. Str. (MPa)
861002	213701.0	53.81	161.24	020	12.1	4.7	15.93	−014	03.1
870214	164219.3	54.66	161.95	032	13.1	5.7	16.83	+108	04.3
870413	021659.7	54.51	161.98	022	11.6	5.0	16.70	−017	00.2
871001	032449.9	54.24	162.69	056	11.8	5.0	15.95	+092	02.7
871023	005946.7	52.88	160.11	035	12.3	5.5	16.53	+127	01.6
871206	181636.0	54.45	161.69	032	12.7	5.4	16.37	+132	05.7
871213	121528.1	51.77	158.92	038	12.6	5.3	16.62	+119	03.9
880111	210731.4	54.62	161.81	042	13.3	5.8	16.94	+092	08.9
880203	094347.5	51.39	161.33	040	12.0	5.1	16.77	+151	00.7
880204	024432.4	52.82	160.12	029	12.3	5.4	16.53	+098	01.5
880209	202707.3	52.66	160.96	012	11.5	5.1	16.51	−044	00.2
880312	083854.2	54.63	161.85	040	13.2	5.7	16.58	+092	16.1
880523	185108.3	52.36	159.17	042	11.7	5.0	16.65	+086	00.4
880812	194258.1	52.48	160.74	009	11.6	4.8	16.55	−022	00.2
880902	102746.4	53.81	161.54	020	12.8	5.1	17.31	+121	00.7
881012	180440.4	53.70	161.22	027	12.1	5.2	16.62	+117	00.8
881017	055650.5	51.16	159.57	015	12.8	5.5	17.52	−009	00.4
881215	092119.8	51.04	158.10	022	12.6	5.3	16.59	+127	03.1
890502	230109.8	53.71	160.74	032	11.5	5.3	16.49	+163	00.3
890522	110802.5	53.61	161.65	000	11.6	5.0	17.25	+135	00.04
890616	041947.5	52.30	159.63	032	11.7	4.9	16.24	+126	00.8
890708	093158.1	52.70	160.20	028	12.3	5.5	16.15	+133	03.8
908718	104115.5	53.24	160.72	051	11.7	5.4	16.62	+133	00.5
890915	183415.4	53.19	160.01	044	13.0	5.6	16.91	+097	04.7
900301	022323.6	53.29	160.23	024	13.5	5.4	17.87	+151	01.1
900310	101505.2	50.74	157.54	026	13.2	5.7	16.79	+110	06.7
900511	050329.2	51.32	159.87	040	12.1	5.0	16.65	−082	01.1
901001	065906.6	52.73	160.55	000	12.2	4.9	16.02	+012	02.5
901219	134825.8	52.77	160.65	024	13.5	5.9	17.84	+091	01.2
901226	153201.9	52.80	160.72	030	11.9		17.14	−055	00.2
901228	014235.1	52.74	160.86	009	12.9	5.1	16.71	−038	02.6
901228	074009.9	52.68	161.13	015	12.7	5.1	17.02	+104	01.1
910504	124056.6	51.94	158.93	040	12.1		16.45	+099	04.1
910604	160245.1	53.34	161.64	035	12.1	5.2	17.28	±006	00.2
910610	063945.9	52.46	160.88	014	11.9	5.0	17.11	+168	00.1
910615	170154.5	52.62	160.58	012	11.7	5.0	16.84	+163	00.2
910708	211423.4	53.04	160.29	034	12.3	5.4	16.38	+120	02.1
910806	202627.5	54.59	161.83	040	11.9	5.5	16.06	+103	01.8
910811	121825.3	52.41	159.54	029	12.6	5.0	17.10	−005	00.7